ECCOMAS Congress 2016
VII European Congress on Computational Methods in Applied Sciences and Engineering
M. Papadrakakis, V. Papadopoulos, G. Stefanou, V. Plevris (eds.)
Crete Island, Greece, 5–10 June 2016

MODELLING CONTACT IN ROCKING STRUCTURES WITH A NONSMOOTH DYNAMICS APPROACH

Anastasios I. Giouvanidis[1], **Elias G. Dimitrakopoulos**[2]

[1]Department of Civil and Environmental Engineering, The Hong Kong University of Science and Technology
Kowloon Bay, Hong Kong
e-mail: agiouvanidis@connect.ust.hk

[2] Department of Civil and Environmental Engineering, The Hong Kong University of Science and Technology
Kowloon Bay, Hong Kong
e-mail: ilias@ust.hk

Keywords: rocking, nonsmooth dynamics, linear complementarity problem, impact, flexible rocking structures.

Abstract. *Rocking action isolates the structure from excessive lateral loads and relieves it from deformation and damage. A complete description of the dynamics of a rocking structure entails, apart from the equation of motion, an appropriate treatment of the contact phenomenon. To date, most analytical and numerical investigations of rocking behavior treat contact with the classical impact model or with ad-hoc assumptions. This paper revisits the contact process adopting a nonsmooth dynamics approach. More specifically, it treats impact through a system of inequalities, which is known as the linear complementarity problem (LCP). Throughout the study, impact is considered to be instantaneous. Set-valued contact laws model the behavior in the normal direction of the (unilateral) contact. The analysis assumes that sliding in the tangential direction is prevented. The present study demonstrates the ability of the proposed methodology to capture the impact behavior of different structures rocking on a rigid base. The results show that the proposed LCPs verify the corresponding results of other methodologies. In addition, the proposed nonsmooth dynamics approach offers a more concise description of the impact problem in rocking structures and it contributes to a more realistic treatment and better understanding of the contact phenomenon during rocking.*

1 INTRODUCTION

Rocking action relieves the structure from deformation and damage during strong earthquakes, offering a favorable seismic isolation effect (e.g.[15]). As a consequence, it attracts the attention of researchers which examine the dynamic behavior of rocking structures either experimentally [17] or analytically [25, 10, 24, 28]. While most studies ignore the (e.g. flexural) deformation of the rocking structures, [6, 23] studied the dynamics of flexible (deforming) rocking structures. Those studies compared flexible base-fixed structures with flexible structures allowed to uplift, and showed that in most cases base-fixed structures sustain larger deformations than rocking structures, verifying the earlier results of [19]. They also highlighted the sensitivity of the characteristics of the rocking systems and of the excitation considered on the response. Recent studies [20, 1, 2, 29, 27] revisited the stability of flexible rocking structures sustaining large rotations. They unveiled that for large flexible rocking structures, the effect of flexibility is not detrimental to the stability.

However, a complete description of the dynamics of a rocking structure requires, apart from the equation of motion, an appropriate treatment of the impact. During rocking, the motion of the structure is interrupted by nonsmooth impacts at the contact points. To date, most analytical studies on the rocking behavior treat impacts with ad-hoc assumptions which usually hinge on the conservation of angular momentum (e.g. [15, 18, 12, 13]). The classical approach results in a coefficient of restitution, usually defined as the angular velocity ratio after and before impact [15], which provides the unknown post-impact state. While such approach can provide dependable results for very simple rigid rocking structures, the investigation of progressively more realistic and more complicated rocking structures, creates incentive for more sophisticated analysis/simulation methods of the involved contact/impact phenomenon. More systematic approaches have been proposed in the context of nonsmooth dynamics [4, 14, 16, 21] or finite elements [26]. These methodologies rely on either a rigid multibody approach [5], or assume deformable contact formulations [3], or utilize compliant contact elements between the contacting bodies [30].

The present study describes the impact event adopting a nonsmooth dynamics approach. The aim of this paper is (i) to present briefly the nonsmooth approach, (ii) to treat impact (without sliding) between unilateral contacts and (iii) to evaluate its implementation to various rocking structures.

2 PROPOSED NONSMOOTH ANALYSIS APPROACH

2.1 Nonsmooth dynamics

The proposed herein nonsmooth dynamics approach assumes that the response can be decomposed into *smooth motion* and *nonsmooth events* [4, 14, 16, 8, 9, 11]. The present study examines the impact phenomenon in two archetypal rocking structures (Fig. 2): (i) the rigid block, and (ii) the flexible oscillator. The proposed approach originates from multibody dynamics with unilateral contacts [22, 16]. Specifically, impact, between rigid bodies which cannot overlap (impenetrability constraint), is considered instantaneous. Subsequently, all non-impulsive forces are considered negligible. Under these assumptions, instantaneous contacts (i.e. impacts) induce sudden, velocity changes ("jumps") making the response discontinuous (nonsmooth). The focus of the present study is on structures designed to exhibit planar rocking. Hence, this study assumes that sliding between contacting bodies is prevented, either by proper detailing of the contact connections to act as shear keys or by sufficient friction coefficient.

2.2 Linear complementarity problem (LCP) for impact

In general, the LCP is based on determining from a system of linear equations $\mathbf{y} = \mathbf{A}\mathbf{x} + \mathbf{b}$, with the matrices $\mathbf{A}$ and $\mathbf{b}$ known, the two unknown non-negative vectors $\mathbf{x} \geq 0$ and $\mathbf{y} \geq 0$ satisfying the complementarity condition: $\mathbf{y}^T\mathbf{x} = 0$. The LCP encapsulates a great variety of contact states, such as impact, "flight" (detachment/separation), bouncing and full contact [4].

The (Newton-Euler) equation of motion for a multibody system with unilateral contacts can be written as:

$$\mathbf{M}\ddot{\mathbf{q}} - \mathbf{h}(\mathbf{C}, \mathbf{K}, \ddot{u}_g(t)) - \mathbf{W}_N\lambda_N - \mathbf{W}_T\lambda_T = \mathbf{0} \tag{1}$$

where $\mathbf{q}$ is the generalized coordinates vector. $\mathbf{M}$, $\mathbf{C}$ and $\mathbf{K}$ are the mass, the damping and the stiffness matrices respectively, and $\mathbf{h}$ is the vector containing all the non-impulsive forces e.g. external excitation ($\ddot{u}_g(t)$), dissipating and elastic forces. $\mathbf{W}$ are the direction matrices of the contact forces in the normal (subscript '*N*') and the tangential (subscript '*T*') direction of contact respectively, and λ are the pertinent contact force vectors. To capture the impact-induced velocity jumps, we integrate the equation of motion (Eq. (1)) over the time interval of impact. Let t^- (and superscript $^-$) and t^+ (and superscript $^+$) denote the time at the beginning and at the end of impact respectively.

$$\lim_{t^-\to t^+}\int_{t^-}^{t^+}\mathbf{h}(\mathbf{C}, \mathbf{K}, \ddot{u}_g)dt = \mathbf{0}, \quad \lim_{t^-\to t^+}\int_{t^-}^{t^+}\lambda_N dt = \mathbf{\Lambda}_N, \quad \lim_{t^-\to t^+}\int_{t^-}^{t^+}\lambda_T dt = \mathbf{\Lambda}_T \tag{2}$$

Eq. (1) becomes:

$$\dot{\mathbf{q}}^+ + \dot{\mathbf{q}}^- = \mathbf{M}^{-1}\mathbf{W}_N\mathbf{\Lambda}_N + \mathbf{M}^{-1}\mathbf{W}_T\mathbf{\Lambda}_T \tag{3}$$

where vector $\dot{\mathbf{q}}$ denotes the generalized velocities. Pre-multiplying Eq. (3) by $\mathbf{W}_N^T$ (and $\mathbf{W}_T^T$) returns the vectors of the relative contact velocities in the normal $\dot{\mathbf{g}}_N = \mathbf{W}_N^T\dot{\mathbf{q}}$ (and in the tangential $\dot{\mathbf{g}}_T = \mathbf{W}_T^T\dot{\mathbf{q}}$) direction accordingly:

$$\begin{aligned}\dot{\mathbf{g}}_N^+ - \dot{\mathbf{g}}_N^- &= \mathbf{G}_{NN}\mathbf{\Lambda}_N + \mathbf{G}_{NT}\mathbf{\Lambda}_T \\ \dot{\mathbf{g}}_T^+ - \dot{\mathbf{g}}_T^- &= \mathbf{G}_{TN}\mathbf{\Lambda}_N + \mathbf{G}_{TT}\mathbf{\Lambda}_T\end{aligned} \tag{4}$$

where the $\mathbf{G}$ matrices are:

$$\begin{aligned}\mathbf{G}_{NN} &= \mathbf{W}_N^T\mathbf{M}^{-1}\mathbf{W}_N, \quad \mathbf{G}_{NT} = \mathbf{W}_N^T\mathbf{M}^{-1}\mathbf{W}_T \\ \mathbf{G}_{TN} &= \mathbf{W}_T^T\mathbf{M}^{-1}\mathbf{W}_N, \quad \mathbf{G}_{TT} = \mathbf{W}_T^T\mathbf{M}^{-1}\mathbf{W}_T\end{aligned} \tag{5}$$

This study assumes that sliding is prevented, therefore the tangential relative (contact) velocity is zero $\dot{\mathbf{g}}_T = \mathbf{0}$, and Eq. (4) gives:

$$\mathbf{\Lambda}_T = -\mathbf{G}_{TT}^{-1}\mathbf{G}_{TN}\mathbf{\Lambda}_N \tag{6}$$

Newton's impact law : Newton's law defines the ratio of the relative normal contact velocities, before ($\dot{g}_N^-$) and after impact ($\dot{g}_N^+$), as the coefficient of restitution ε_N:

$$\dot{\mathbf{g}}_N^+ = -\bar{\bar{\varepsilon}}_N\dot{\mathbf{g}}_N^- \tag{7}$$

$\bar{\bar{\varepsilon}}_N$ is the diagonal matrix of the dissipative coefficient of restitution ε_N, and varies from zero for perfectly inelastic (plastic) impact to one for perfectly elastic impact. The velocity jump along the normal direction of impact is:

$$\mathbf{v}_N = \dot{\mathbf{g}}_N^+ + \bar{\bar{\varepsilon}}_N\dot{\mathbf{g}}_N^- \tag{8}$$

then, Eq. (4) yields a system of linear equations:

$$\mathbf{v}_N = \left(\mathbf{G}_{NN} - \mathbf{G}_{NT}\mathbf{G}_{TT}^{-1}\mathbf{G}_{TN}\right)\mathbf{\Lambda}_N + \left(\mathbf{E} + \overline{\overline{\varepsilon}}_N\right)\dot{\mathbf{g}}_N^- \tag{9}$$

for which the additional complementarity conditions hold:

$$\mathbf{v}_N \geq \mathbf{0},\ \mathbf{\Lambda}_N \geq \mathbf{0},\ \mathbf{v}_N^T\mathbf{\Lambda}_N = 0 \tag{10}$$

In Eq. (9), $\mathbf{E}$ is the identity matrix. Eqs (9), (10) define a LCP which treats (non-sliding) impacts according to Newton's law. The complementarity conditions (Eq. 10) reflect the inequality character of (dry) contacts. Fig. 1 illustrates this complementary relationship; the positive part of the horizontal axis allows positive normal impulses with zero velocities, while the vertical axis allows positive relative velocities with zero normal impulses.

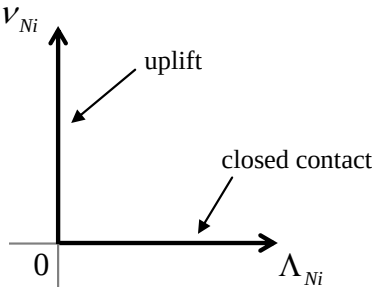

Figure 1: The inequality character of contact [22].

3 REVIEW OF THE ROCKING BLOCK USING THE PROPOSED APPROACH

The present section revisits the impact behavior of the rigid rocking block of Fig. 2(a) adopting the proposed nonsmooth dynamics approach. Consider a rigid block with base width $2b$ and height $2H$ as in Fig. 2(a). The generalized coordinates vector for the planar rocking motion of the block is: $\mathbf{q}^T = \begin{bmatrix} x & y & \phi \end{bmatrix}$, where x and y are the translations along the pertinent axes, and ϕ is the planar rocking rotation. Assume that the two closed contact points (pivot points "1" and "2") produce two forces/impulses in the normal direction of contact (one force per point), but only one force in the tangential direction of contact, the resultant of the two tangential forces at the two pivot points (e.g. as in Fig. 3). The consideration of the resultant tangential force (instead of its constituents) is eligible by the rigid body assumption (the two constituents are linearly dependent) and most importantly, does not overconstraint the problem [8, 9, 11]. Thus, the mass matrix and the direction matrices in the normal and tangential direction of contact become respectively:

$$\mathbf{M} = \begin{bmatrix} m & 0 & 0 \\ 0 & m & 0 \\ 0 & 0 & I_0 \end{bmatrix},\ \mathbf{W}_N = \begin{bmatrix} 0 & 0 \\ 1 & 1 \\ -b & b \end{bmatrix},\ \mathbf{W}_T = \begin{bmatrix} 1 \\ 0 \\ H \end{bmatrix} \tag{11}$$

where I_0 is the mass moment of inertia with respect to the center of mass of the block. For a rectangular block $I_0 = (1/3)\,mR^2$, where m is the mass of the block and R is the half diagonal distance (Fig. 2(a)).

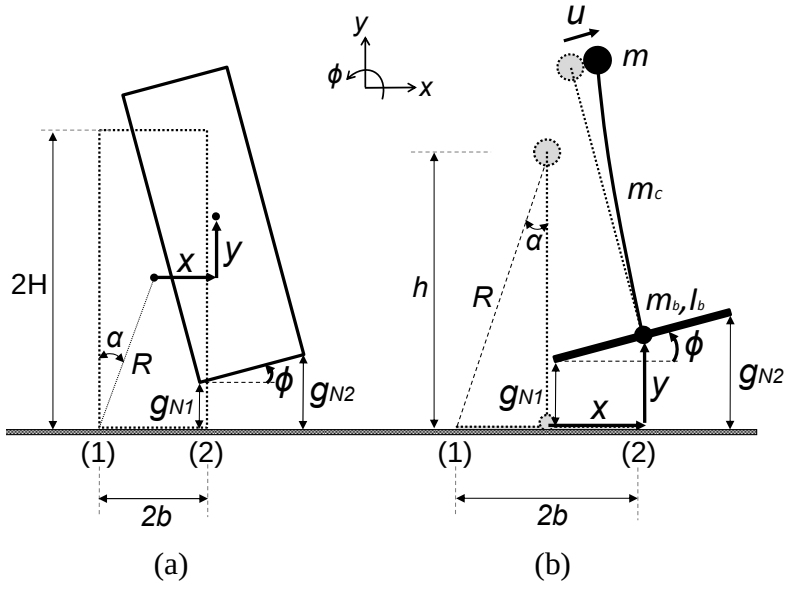

Figure 2: The examined rocking structures: (a) rigid block, (b) flexible oscillator.

3.1 Analysis of all physically feasible post-impact states

With reference to Fig. 3, consider a rigid block performing pure rotation (without sliding) about pivot point "1" ($g_{N1}^- = \dot{g}_{N1}^- = 0$). Impact takes place at pivot point "2" at the moment $g_{N2}^- = 0$ and with pre-impact contact velocity $\dot{g}_{N2}^- = 2b\dot{\phi}^- < 0$. There are four possible (post-impact) states (Fig. 3(E)): (i) full contact ($E_{1/1}$), (ii) bouncing ($E_{1/2}$), (iii) rocking ($E_{2/1}$), and (iv) "flight" ($E_{2/2}$). This section examines all physically feasible post-impact states, and determines the conditions under which each (post-impact) state occurs.

Full contact ($A \to E_{1/1}$) or bouncing ($A \to E_{1/2}$) (Fig. 3): When after impact, point "1" remains in contact with the ground ($\dot{g}_{N1}^+ = 0$), point "2" might stay in contact or not ($\dot{g}_{N2}^+ \geq 0$). The corresponding velocity jumps at the two contact points are (Eqs (7), (8)):

$$\begin{aligned} \nu_{N1} &= \dot{g}_{N1}^+ + \varepsilon_N \dot{g}_{N1}^- = \dot{g}_{N1}^+ = 0 \\ \nu_{N2} &= \dot{g}_{N2}^+ + \varepsilon_N \dot{g}_{N2}^- = -\varepsilon_N \dot{g}_{N2}^- + \varepsilon_N \dot{g}_{N2}^- = 0 \end{aligned} \tag{12}$$

Eq. (12) implies that the block bounces at point "2" with a contact velocity $\dot{g}_{N2}^+ = -\varepsilon_N \dot{g}_{N2}^- > 0$ for a nonzero (Newton) coefficient of restitution $\varepsilon_N > 0$, and it stays in full contact at point "2" ($\dot{g}_{N2}^+ = 0$) for $\varepsilon_N = 0$. In either case, both velocity jumps are zero (Eq. (12)) and thus known. It follows (Eq. 10) that the remaining two unknowns, the normal impulses Λ_{N1} and Λ_{N2}, are both positive. The solution of the LCP of Eq. (9) yields their values:

$$\begin{aligned} \frac{\Lambda_{N1}}{m\dot{g}_{N2}^-} &= (1+\varepsilon_N)\left(\frac{1}{3\sin^2\alpha} - \frac{1}{2}\right) \\ \frac{\Lambda_{N2}}{m\dot{g}_{N2}^-} &= -(1+\varepsilon_N)\frac{1}{3\sin^2\alpha} \end{aligned} \tag{13}$$

with the help of which, Eq. (6) gives the (dimensionless) tangential impulse:

$$\frac{\Lambda_T}{m\dot{g}_{N2}^-} = (1+\varepsilon_N)\frac{\cot\alpha}{2} \tag{14}$$

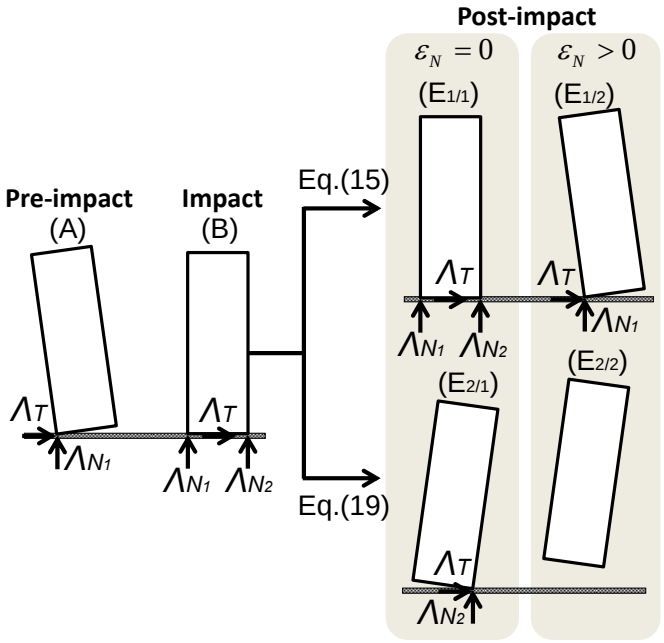

Figure 3: Post-impact states for the rocking block according to Newton's law.

Note that, all unknowns (contact velocities and/or impulses) are given in dimensionless terms.

The inequality character of contact determines the (existential) conditions under which each post-impact state occurs. Specifically, the $\Lambda_{N1} > 0$ condition and Eq. (13) show that the block can bounce or remain in full contact with the ground after impact when:

$$\frac{H}{b} < \frac{1}{\sqrt{2}} \tag{15}$$

in agreement with [5].

Rocking ($A \rightarrow E_{2/1}$) or "flight" ($A \rightarrow E_{2/2}$) (Fig. 3): Assume that after impact the block changes pivot point. Hence, contact at point "1" is lost $\dot{g}_{N1}^{+} > 0$, while the new contact at point "2" is either maintained $\dot{g}_{N2}^{+} = 0$, or also lost $\dot{g}_{N2}^{+} > 0$. The velocity jumps for the two contact points are (Eqs (7), (8)):

$$\begin{aligned} \nu_{N1} &= \dot{g}_{N1}^{+} + \varepsilon_N \dot{g}_{N1}^{-} = \dot{g}_{N1}^{+} > 0 \\ \nu_{N2} &= \dot{g}_{N2}^{+} + \varepsilon_N \dot{g}_{N2}^{-} = 0 \end{aligned} \tag{16}$$

The velocity jumps of Eq. (16) give $0 = \nu_{N2} = \varepsilon_N \dot{g}_{N2}^{-}$. When ε_N is nonzero, contact at point "2" is lost ($\dot{g}_{N2}^{+} = -\varepsilon_N \dot{g}_{N2}^{-} > 0$) and uplifting (detachment) of both contact points takes place. The former case ($\varepsilon_N = 0$) leads to pure rocking behavior while the latter ($\varepsilon_N > 0$) to "flight" behavior. For velocity jumps $\nu_{N1} > 0$ and $\nu_{N2} = 0$, the complementarity conditions (Eq. (10)) return $\Lambda_{N1} = 0$ and $\Lambda_{N2} > 0$. The solution of the LCP of Eq. (9) yields the remaining two unknowns, the normal impulse Λ_{N2} at point "2", and the post-impact normal contact velocity $\dot{g}_{N1}^{+}$ of point "1":

$$\begin{aligned} \frac{\Lambda_{N2}}{m\dot{g}_{N2}^{-}} &= (1+\varepsilon_N)\left(\frac{3\sin^2\alpha}{4} - 1\right) \\ \frac{\dot{g}_{N1}^{+}}{\dot{g}_{N2}^{-}} &= (1+\varepsilon_N)\left(\frac{3\sin^2\alpha}{2} - 1\right) \end{aligned} \tag{17}$$

and from Eq. (6), the tangential impulse becomes:

$$\frac{\Lambda_T}{m\dot{g}_{N2}^-} = \frac{3}{4}(1+\varepsilon_N)\sin\alpha\cos\alpha \tag{18}$$

Again, the inequality character of contact dictates the (existential) conditions under which each post-impact state occurs. Specifically, when contact at point "1" is lost ($\Lambda_{N1} = 0$), the complementary behavior (Fig. 1) requires $\dot{g}_{N1}^+ > 0$. Hence, Eq. (17) shows that the block exhibits rocking or "flight" post-impact behavior when [5]:

$$\frac{H}{b} > \frac{1}{\sqrt{2}} \tag{19}$$

In summary, Eqs (12) to (19) describe completely all possible post-impact states for the rigid rocking block. Thus, the proposed methodology verifies the corresponding results from other methodologies, while at the same time encapsulates all physically feasible post-impact states. Specifically, the geometric slenderness criterion, derived by [5], is in agreement with Eqs (15), (19). For non-sliding (sticking) impacts, a rocking block is considered "stocky" when Eq. (15) is satisfied, whereas when Eq. (19) holds, the block is regarded as "slender". In many studies, including past work of the authors ([10, 7, 12, 13] among others), the ratio $\eta = \dot{\phi}^+ \big/ \dot{\phi}^-$ defines a coefficient of restitution with respect to the angular velocities. When a (slender) block rocks or separates ("flight" mode) from the ground after impact (Fig. 3($E_{2/1}$/$E_{2/2}$)), Eq. (3) with the aid of Eqs (17), (18) shows that the relationship between pre- and post-impact angular velocity ratio is:

$$\eta = \frac{\dot{\phi}^+}{\dot{\phi}^-} = 1 - \frac{3}{2}\sin^2\alpha - \frac{3}{2}\varepsilon_N\sin^2\alpha \tag{20}$$

Eq. (20) verifies the pertinent equation derived by [25, 17]. For perfectly inelastic (plastic) impact ($\varepsilon_N = 0$), the block exhibits pure rocking behavior, and Eq. (20) agrees with the Housner's angular coefficient of restitution [15].

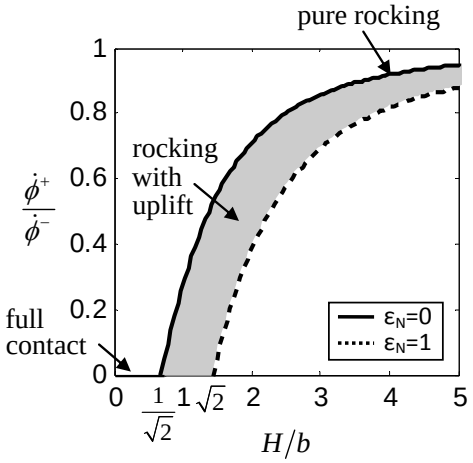

Figure 4: Admissible regions for all the post-impact states for the rocking block.

Eqs (13), (14) treat the bouncing and full contact behavior of the block (Fig. 3($E_{1/1}$/$E_{1/2}$)), with the help of which Eq. (3) gives:

$$\eta = \frac{\dot{\phi}^+}{\dot{\phi}^-} = -\varepsilon_N \tag{21}$$

Eq. (21) shows that for $\varepsilon_N = 0$ the block remains in full contact after impact ($\dot{\phi}^+ \big/ \dot{\phi}^- = 0$), while for perfectly elastic impact ($\varepsilon_N = 1$), the rocking block bounces without any loss of kinetic energy.

Fig. 4 illustrates the admissible regions of all the examined post-impact states of the rigid rocking block. For non-sliding impacts, Fig. 4 shows the admissible domain when rocking occurs. A slender block exhibits pure rocking motion (Eq. (20)) when $\varepsilon_N = 0$. The grey area in Fig. 4 describes the rocking behavior of the block which is accompanied by uplifts/jumps of the pivot points immediately after impact occurs [25, 17]. Note that, the higher the slenderness ratio H/b, the less energy is dissipated during impact, and, in the limit, as this ratio becomes (theoretically) infinite, the block rocks without any energy loss.

4 NUMERICAL EVALUATION OF THE PROPOSED APPROACH

This section illustrates the versatility of the proposed approach by examining (numerically) the behavior of a rigid rocking block and a flexible oscillator in terms of time history analysis (Fig. 2). Consider (i) a stocky block with $2b$ = 1.4 m base width and $H/b = 1\big/\sqrt{2}$ (Eq. (15), Fig. 5(a)) and (ii) a slender block with the same base width but $H/b = 7.0$ (Eq. (19), Fig. 5(b)). The frequency parameter of a rocking block is $p = \sqrt{3g/4R}$, where g is the gravitational acceleration and R is the half-diagonal distance (Fig. 2(a)). Fig. 5 plots the free rocking response of both a stocky and a slender block (Fig. 5(a) and Fig. 5(b) respectively). Specifically, Fig. 5(a)(top) plots the response of the block for three different (Newton) coefficients of restitution. Both blocks have an initial rotation equal with $\alpha/3$, where α denotes the slenderness of the block (Fig. 2(a)). The stocky block does not change pivot point after impact and hence, exhibits bouncing behavior. When $\varepsilon_N = 0$ the impact is considered totally inelastic (plastic) and the block remains in full contact after impact with the ground. On the contrary, for totally elastic impacts ($\varepsilon_N = 1$) the stocky block bounces without any energy loss at impact. The slender block though, changes pivot point after each impact and exhibits pure rocking motion for $\varepsilon_N = 0$ (Fig. 5(b)(top)). Fig. 5(bottom) shows the normal relative distance g_N of the two contact points (as Fig. 2 shows) for both the bouncing and the rocking motion of the two blocks. It is important to note, that both bouncing and rocking behavior are captured numerically with the aid of the same LCP.

Fig. 6 plots the response of the slender rocking block by comparing the proposed nonsmooth dynamics approach for $\varepsilon_N = 0$ with the classical impact model [15] assuming an angular coefficient of restitution equal with 0.97 (according to Eq. (20)). The two (identical) blocks exhibit pure rocking motion and are subjected to the same sine pulse excitation with $\alpha_g/g = 0.45$ and $\omega_g/p = 5.75$. Fig. 6 shows that the results derived by the proposed methodology are in complete agreement with the classical impact model. In addition, the proposed methodology encapsulates all physically feasible post impact states; something that is not feasible with the classical impact model.

Further, the proposed approach is also applicable to more complicated rocking structures. Consider the flexible rocking oscillator of Fig. 2(b) with slenderness $\alpha = 0.1\ rad$ and $H/b = 10$ [29]. The oscillator has a deformable column with mass m_c uniformly distributed along its length. Assume the concentrated (lumped) mass m on the top has zero moment of inertia, whereas the base mass m_b gives moment of inertia $I_b = (1/3)\, m_b b^2$ with respect to its center of mass. The generalized coordinates vector for the planar rocking motion of the flexible rocking oscillator is: $\mathbf{q}^T = \begin{bmatrix} u & x & y & \phi \end{bmatrix}$, where x and y are the translations of the base mass along the pertinent axes, u is the elastic relative translation of the lumped mass and ϕ is the planar

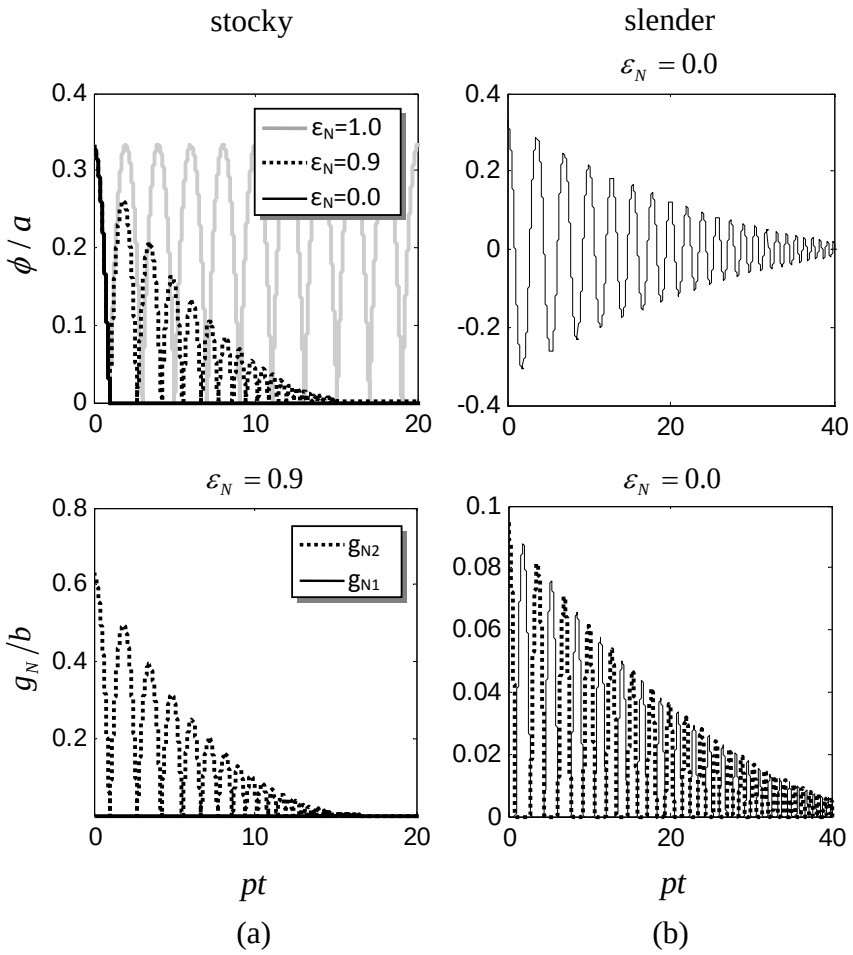

Figure 5: Free rocking response for (a) a stocky and (b) a slender block.

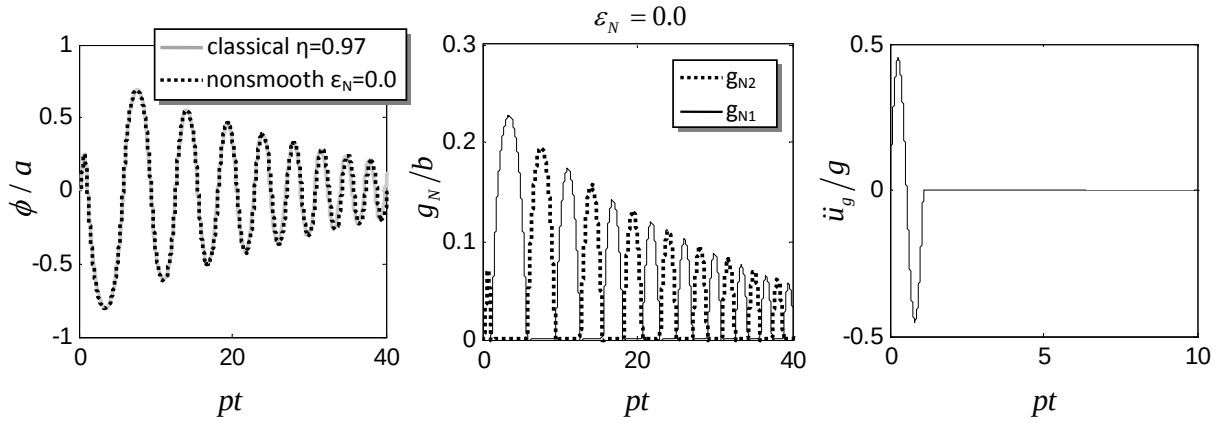

Figure 6: Comparison between the nonsmooth dynamics approach and the classical impact model for a (slender) rocking block subjected to sine pulse with $\alpha_g = 0.45g$ and $\omega_g = 5.75p$.

rocking rotation (Fig. 2(b)). Following [29], the present study assumes $\gamma_{m_b} = m_b/m = 2$ and $\gamma_{m_c} = m_c/m = 1$. Further, the damping ratio is taken as 1%, while the natural frequency ω_n/p is considered as 5, with p being the frequency parameter of the oscillator equal with $p = \sqrt{g/R}$.

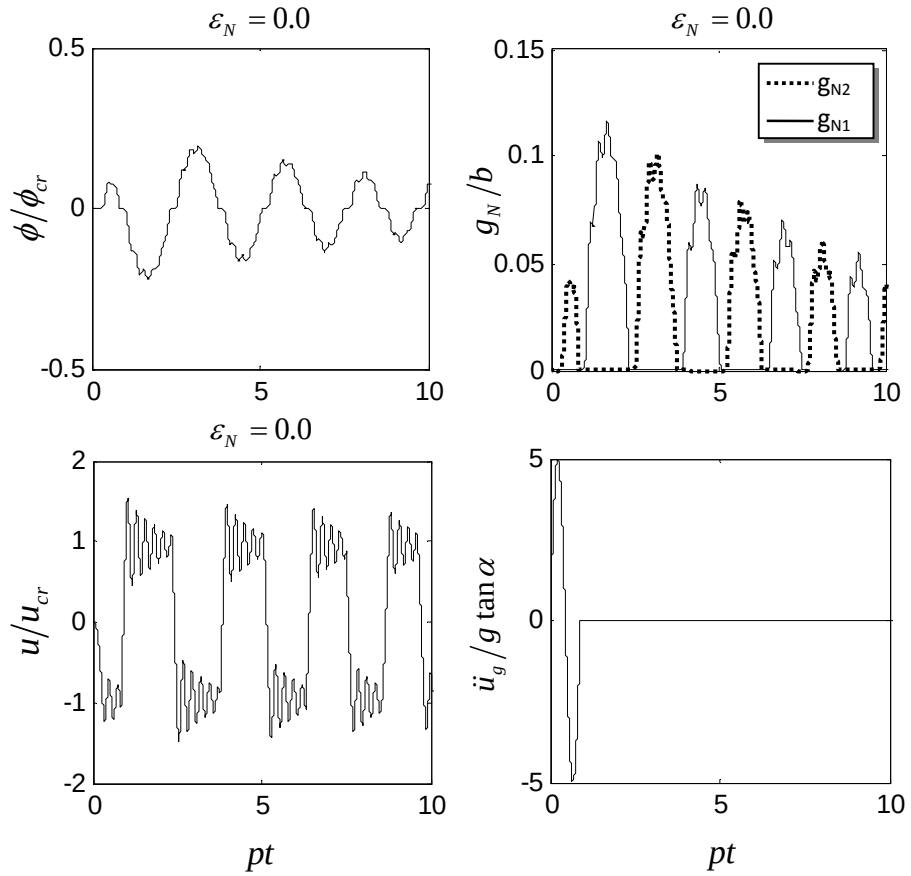

Figure 7: Time history response of the (slender) flexible rocking oscillator subjected to sine pulse with $\alpha_g = 5g\tan\alpha$ and $\omega_g = 7p$.

Fig. 7 shows that subjected to a sine pulse excitation with $\alpha_g/g\tan\alpha = 5$ and $\omega_g/p = 7$, the flexible rocking oscillator of Fig. 2(b) exhibits pure rocking motion, which is in good agreement with the pertinent results from [29]. Note that, ϕ_{cr} denote the "critical" rocking angle of unstable equilibrium for the rigid rocking oscillator, and u_{cr} the "critical" relative displacement of the mass m at the time-instant rocking initiates [29].

5 CONCLUSIONS

The present study revisits the contact/impact phenomenon encountered in rocking structures adopting a nonsmooth dynamics approach. In particular, it formulates the impact problem as a system of inequalities, known as linear complementarity problem (LCP), and examines the impact of two archetypal rocking structures: the rigid rocking block and the flexible rocking oscillator. In the normal direction of contact, the present analysis adopts the Newton's contact law, while in the tangential direction sliding is prevented (non-sliding contact). The analysis shows that the results from the proposed LCPs are in total agreement with the pertinent results

of other methodologies. Overall, this work demonstrates the ability of the proposed nonsmooth dynamics approach to capture all physically feasible post-impact states in a systematic and condensed manner; at least for the rocking systems examined.

6 ACKNOWLEDGMENTS

Financial support was provided by the Research Grants Council of Hong Kong, under grant reference number ECS 639613.

REFERENCES

[1] Acikgoz, S., DeJong, M. J., The interaction of elasticity and rocking in flexible structures allowed to uplift. *Earthquake Engineering & Structural Dynamics*, **41**(15), 2177–2194, 2012.

[2] Acikgoz, S., DeJong, M. J., The rocking response of large flexible structures to earthquakes. *Bulletin of earthquake engineering*, **12**(2), 875–908, 2014.

[3] Andreaus, U., Casini, P., Dynamics of three-block assemblies with unilateral deformable contacts. Part 1: contact modelling. *Earthquake engineering & structural dynamics*, **28**(12), 1621–1636, 1999.

[4] Brogliato, B., *Nonsmooth mechanics: models, dynamics and control*. Springer, 1999.

[5] Brogliato, B., Zhang, H., Liu, C., Analysis of a generalized kinematic impact law for multibody-multicontact systems, with application to the planar rocking block and chains of balls. *Multibody System Dynamics*, **27**(3), 351–382, 2012.

[6] Chopra, A. K., Yim, S. C. S., Simplified earthquake analysis of structures with foundation uplift. *Journal of Structural Engineering*, **111**(4), 906–930, 1985.

[7] DeJong, M. J., Dimitrakopoulos, E. G., Dynamically equivalent rocking structures. *Earthquake Engineering & Structural Dynamics*, **43**(10), 1543–1563, 2014.

[8] Dimitrakopoulos, E. G., Analysis of a frictional oblique impact observed in skew bridges. *Nonlinear Dynamics*, **60**(4), 575–595, 2010.

[9] Dimitrakopoulos, E. G., Seismic response analysis of skew bridges with pounding deck-abutment joints. *Engineering Structures*, **33**(3), 813–826, 2011.

[10] Dimitrakopoulos, E. G., DeJong, M. J., Revisiting the rocking block: closed-form solutions and similarity laws. *Proceedings of the Royal Society A: Mathematical, Physical and Engineering Science*, **468**(2144), 2294–2318, 2012.

[11] Dimitrakopoulos, E. G., Nonsmooth analysis of the impact between successive skew bridge-segments. *Nonlinear Dynamics*, **74**(4), 911–928, 2013.

[12] Dimitrakopoulos, E. G., Giouvanidis, A. I., Seismic response analysis of the planar rocking frame. *Journal of Engineering Mechanics*, **141**(7), 04015003, 2015.

[13] Giouvanidis, A. I., Dimitrakopoulos, E. G., Seismic performance of rocking frames with flag-shaped hysteretic behavior. *Journal of Engineering Mechanics*, **under review**, 2016.

[14] Glocker, C., *Set-valued force laws: dynamics of non-smooth systems*. Springer, 2001.

[15] Housner, G. W., The behavior of inverted pendulum structures during earthquakes. *Bulletin of the seismological society of America*, **53**(2), 403–417, 1963.

[16] Leine, R. I., Van Campen, D. H., Glocker, C. H., Nonlinear dynamics and modeling of various wooden toys with impact and friction. *Journal of vibration and control*, **9**(1-2), 25–78, 2003.

[17] Lipscombe, P. R., Pellegrino, S., Free rocking of prismatic blocks. *Journal of engineering mechanics*, **119**(7), 1387–1410, 1993.

[18] Makris, N., Vassiliou, M. F., Planar rocking response and stability analysis of an array of free-standing columns capped with a freely supported rigid beam. *Earthquake Engineering & Structural Dynamics*, **42**(3), 431–449, 2012.

[19] Meek, J. W., Effects of foundation tipping on dynamic response. *Journal of the Structural Division*, **101**(7), 1297–1311, 1975.

[20] Oliveto, G., Calio, I., Greco, A., Large displacement behaviour of a structural model with foundation uplift under impulsive and earthquake excitations. *Earthquake engineering & structural dynamics*, **32**(3), 369–393, 2003.

[21] Payr, M., Glocker, C., Oblique frictional impact of a bar: analysis and comparison of different impact laws. *Nonlinear Dynamics*, **41**(4), 361–383, 2005.

[22] Pfeiffer, F., Glocker, C., *Multibody dynamics with unilateral contacts*. Springer Science & Business Media, 2000.

[23] Psycharis, I. N., Effect of base uplift on dynamic response of SDOF structures. *Journal of Structural Engineering*, **117**(3), 733–754, 1991.

[24] Psycharis, I. N., Fragiadakis, M., Stefanou, I., Seismic reliability assessment of classical columns subjected to near-fault ground motions. *Earthquake Engineering & Structural Dynamics*, **42**(14), 2061–2079, 2013.

[25] Shenton III, H. W., Jones, N., P., Base excitation of rigid bodies. I: Formulation. *Journal of Engineering Mechanics*, **117**(10), 2286–2306, 1991.

[26] Theodosiou, C., Natsiavas, S., Dynamics of finite element structural models with multiple unilateral constraints. *International Journal of Non-Linear Mechanics*, **44**(4), 371–382, 2009.

[27] Truniger, R., Vassiliou, M. F., Stojadinovic B., An analytical model of a deformable cantilever structure rocking on a rigid surface: experimental validation. *Earthquake Engineering & Structural Dynamics*, **44**(15), 2795–2815, 2015.

[28] Vassiliou, M. F., Mackie, K. R., Stojadinovic B., Dynamic response analysis of solitary flexible rocking bodies: modeling and behavior under pulse-like ground excitation. *Earthquake Engineering & Structural Dynamics*, **43**(10), 1463–1481, 2014.

[29] Vassiliou, M. F., Truniger, R., Stojadinovic B., An analytical model of a deformable cantilever structure rocking on a rigid surface: development and verification. *Earthquake Engineering & Structural Dynamics*, **44**(15), 2775–2794, 2015.

[30] Yilmaz, C., Gharib, M., Hurmuzlu, Y., Solving frictionless rocking block problem with multiple impacts. *Proceedings of the Royal Society A: Mathematical, Physical and Engineering Science*, **10.1098/rspa.2009.0273**, 2009.